# Thermal and Fluid Transport in Micro-Open-Cell Metal Foams: Effect of Node Size

**Xiaohu Yang**
Group of the Building Energy & Sustainability Technology,
School of Human Settlements and Civil Engineering,
Xi'an Jiaotong University,
Xi'an 710049, China;
MOE Key Lab for Multifunctional Materials and Structures,
Xi'an Jiaotong University,
Xi'an 710049, China
e-mail: xiaohuyang@xjtu.edu.cn

**Yang Li**
Group of the Building Energy & Sustainability Technology,
School of Human Settlements and Civil Engineering,
Xi'an Jiaotong University,
Xi'an 710049, China

**Lianying Zhang**
Group of the Building Energy & Sustainability Technology,
School of Human Settlements and Civil Engineering,
Xi'an Jiaotong University,
Xi'an 710049, China

**Liwen Jin**[1]
Group of the Building Energy & Sustainability Technology,
School of Human Settlements and Civil Engineering,
Xi'an Jiaotong University,
Xi'an 710049, China
e-mail: lwjin@xjtu.edu.cn

**Wenju Hu**
Beijing Municipal Key Lab of Heating, Gas Supply, Ventilating and Air Conditioning Engineering,
Beijing University of Civil Engineering and Architecture,
Xicheng District,
Beijing 100044, China

**Tian Jian Lu**[1]
MOE Key Lab for Multifunctional Materials and Structures,
Xi'an Jiaotong University,
Xi'an 710049, China;
State Key Laboratory for Strength and Vibration of Mechanical Structures,
Xi'an Jiaotong University,
Xi'an 710049, China
e-mail: tjlu@xjtu.edu.cn

[1]Corresponding authors.

Presented at the 5th ASME 2016 Micro/Nanoscale Heat & Mass Transfer International Conference. Paper No. MNHMT2016-6457.

Contributed by the Heat Transfer Division of ASME for publication in the JOURNAL OF HEAT TRANSFER. Manuscript received June 14, 2016; final manuscript received March 13, 2017; published online August 16, 2017. Assoc. Editor: Chun Yang.

*Open-cell metal foams exhibit distinctive advantages in fluid control and heat transfer enhancement in thermal and chemical engineering. The thermofluidic transport characteristics at pore scale such as topological microstructure and morphological appearance significantly affect fluid flow and conjugated heat transfer in open-cell metal foams, important for practically designed applications. The present study employed an idealized tetrakaidecahedron unit cell (UC) model to numerically investigate the transport properties and conjugated heat transfer in highly porous open-cell metal foams (porosity—0.95). The effects of foam ligaments and nodes (size and cross-sectional shape) on thermal conduction, fluid flow, and conjugated heat transfer were particularly studied. Good agreement was found between the present predictions and the results in open literature. The effective thermal conductivity was found to decrease with increasing node-size-to-ligament ratio, while the permeability and volume-averaged Nusselt number were increased. This indicated that the effects of node size and shape upon thermofluidic transport need to be considered for open-cell metal foams having high porosities.*
[DOI: 10.1115/1.4037394]

*Keywords: open-cell metal foam, transport phenomena, pore-scale study, direct numerical simulation, node size effect*

## Introduction

Open-cell metallic foams possess distinctive properties such as relatively low manufacturing cost, ultralow density, and high surface area-to-volume ratio, and hence have been utilized in a wide range of applications (e.g., microelectronics cooling [1], fuel cells [2], and compact heat exchangers [3–6]). For such applications, the knowledge of thermal and fluid transport characteristics for metal foams is a key issue, enabling control of fluid flow, heat transfer enhancement, planning and designing chemical engineering processes, optimal flow analysis, as well as practical design [3–8].

To model the thermal and fluid transport in porous media, direct numerical simulation on the reconstructed metal foam structural model is capable of providing physical insight view of pore-scaled features. The work of Boomsma et al. [9] was one of the representative attempts to model the cellular foam topology as a periodic cell structure for fluid and thermal transport in open-cell metal foams. A representative elementary volume deduced from a Kelvin cell (tetrakaidecahedron) was found to have a proper compatibility with the real foam geometry by subsequent investigations [10–14]. Krishnan et al. [15] computed the effective thermal conductivity and permeability by assuming the pores to be spherical and compared different types of packing arrangement for modeling foam geometry—body centered cubic, face centered cubic, and the A15 lattice [16]. Huu et al. [17] employed the pentagonal dodecahedron geometry to model mass transfer in open-cell metal foams to illustrate the effect of foam ligament shape (e.g., slender triangular or cylindrical rods) upon pressure drop. Lucci et al. [18] reconstructed the foam geometry as randomly packed Kelvin cells and conducted simulations on mass transfer. Their numerical results showed good agreement with other investigations, indicating that packaging pattern may have little influence on mass transfer. Zafari et al. [19] modeled convective heat transfer within the range of Reynolds number 20–4500 using idealized tetrakaidecahedron unit cell (UC) model for open-cell foams and demonstrated that such unit cell modeling could enjoy good precision. Cunsolo et al. [13] investigated the effect of foam ligament shape on radiative heat transfer and compared the Kelvin and Weaire–Phelan geometric models in terms of hydraulic and heat transfer features [14]. Their results indicated that different handling of ligament shape can cause up to 50% difference in numerical model predictions. Consequently, the effect of foam ligament shape cannot be neglected when building foam geometric models from the microscopic point view.

 Copyright © 2018 by ASME 

Downloaded From: https://heattransfer.asmedigitalcollection.asme.org on 02/14/2019 Terms of Use: http://www.asme.org/about-asme/terms-of-use

To conclude the above-mentioned literature review, the cellular morphology of a metal foam with open cells, such as pore diameter, pore uniformity, and ligament shape, significantly affects its fluid flow and conjugated heat transfer performances. Particularly, there exist nodes where foam ligaments join together, and their contribution to effective thermal conductivity has been recognized by Calmidi and Mahajan [20], Bhattacharya et al. [21], Boomsma and Poulikakos [22], and Yang et al. [12]. However, the influence of node size and shape on fluid transport and conjugated heat transfer has not been valued from the pore-scale point of view. The present study, therefore, aimed to study systematically the contribution of node size and shape to fluid transport and conjugated heat transfer in highly porous open-cell metal foams. A modified Kelvin cell was selected as the representative unit cell of the foam, and a series of pore-scaled computational fluid dynamics (CFD) simulations were conducted to obtain effective thermal conductivity, permeability, and conjugated heat transfer. For validation, the direct simulation results were compared with existing experimental and numerical data.

## Numerical Simulations

**Geometric Model.** Open-cell aluminum (Al) foams (Fig. 1(*a*)) were assumed to have the topology of periodically distributed tetrakaidecahedron cells, which was in accordance with the present observation and literature [20]. Each tetrakaidecahedron was consisted of six square and eight hexagonal faces having uniform ligament length (circular or square cross-sectional shape) and thickness, with either cubic or spherical nodes. Accordingly, a series of tetrakaidecahedron UCs were built. Figure 1(*c*) depicted

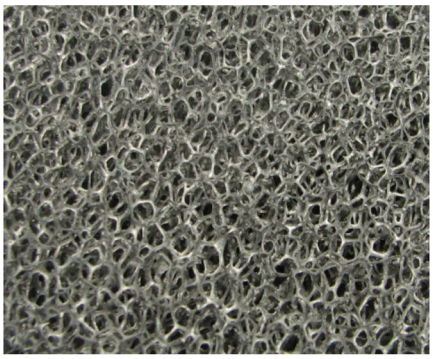

(*a*)

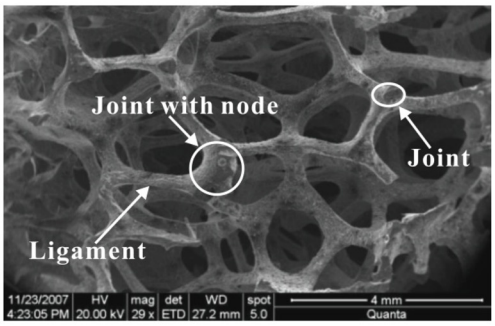


(*b*)

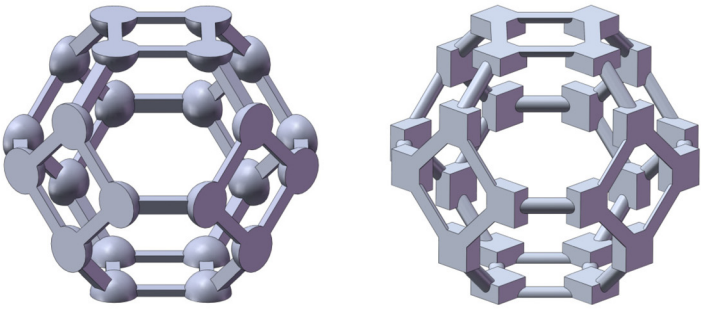

(*c*)

**Fig. 1 (*a*) Highly porous open-celled aluminum (Al) foam fabricated via precision casting, (*b*) scanning electronic microscope image of foam topology, and (*c*) idealized tetrakaidecahedron UC consisted of square cross-sectioned ligaments with spherical nodes and circular cross-sectioned ligaments with cubic nodes**



Downloaded From: https://heattransfer.asmedigitalcollection.asme.org on 02/14/2019 Terms of Use: http://www.asme.org/about-asme/terms-of-use

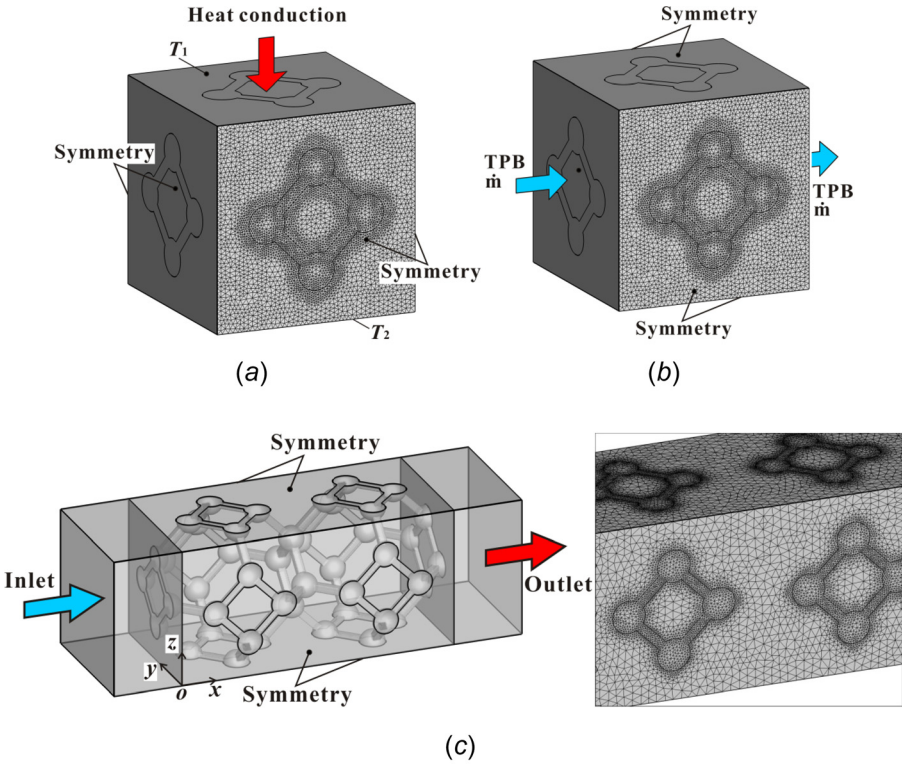


**Fig. 2 Computational domain and representative mesh for (*a*) effective thermal conductivity modeling, (*b*) fluid flow modeling, and (*c*) conjugated heat transfer modeling**

two typical UCs, one having square cross-sectioned ligaments with spherical nodes and the other having circular cross-sectioned ligaments with cubic nodes.

**Representative Mesh.** For modeling effective conductivity and permeability, only one UC was considered (Figs. 2(*a*) and 2(*b*)). For modeling conjugated heat transfer, a computational domain consisting of two UCs and a short inlet and outlet region was built to improve numerical stability (Fig. 2(*c*)). All tetrahedron elements were applied to discretize the three geometrical models, and grid refinement processing was conducted and a three-layer prism mesh was generated as well to improve the mesh quality of the interfaces between ligaments and interstitial fluid. As heat conduction, periodic flow, and conjugated heat transfer are different physical processes, the grid dependence was separately checked in terms of temperature, pressure drop, and volume-averaged Nusselt number. Three different meshes with different tetrahedron elements were employed for CFD computations, and the comparisons were summarized in Table 1. It could be observed from the results of Table 1 that all the predicted values from the last two meshes exhibited a deviation less than 1.4%, favoring the utilization of the finer meshes for all subsequent simulations.

**Initial and Boundary Conditions.** For effective conductivity modeling, the initial temperatures for both the solid and fluid domain were all kept as 293.15 K. The boundary conditions were made as follows (Fig. 2(*a*)): the top and bottom surfaces are kept at constant temperature with $T_1 > T_2$. The other four faces were treated as symmetry.

For permeability modeling, the UC same as the case of effective conductivity modeling was selected, with initial velocity of fluid to be zero. Without considering heat transfer in this case, thus only hydrodynamical boundary conditions were applied: the left and right boundaries were translational periodic boundaries

**Table 1 Simulated flow and heat transfer parameters with different numerical meshes for foam UC with circular ligaments**

| Physical process | Total elements | $T_s$ (K) | $P_{in} - P_{out}$ (Pa) | $Nu_v$ |
|---|---|---|---|---|
| Heat conduction | 495,635 | 332.27 | | |
| | 733,841 | 333.45 | | |
| | 984,452 | 333.47 | | |
| Pressure drop | 495,635 | | 0.5842 | |
| | 733,841 | | 0.5921 | |
| | 984,452 | | 0.5937 | |
| Conjugated heat transfer | 789,135 | 337.164 | 1.1324 | 36.548 |
| | 1,234,879 | 338.022 | 1.1458 | 37.022 |
| | 1,564,894 | 338.139 | 1.1473 | 37.131 |

(Fig. 2(*b*)) with a fixed mass flow rate, enabling thermally and hydrodynamically fully developed flow, while symmetry boundary conditions were applied upon the other four faces.

For conjugated heat transfer modeling, a computational domain consisting of two UCs and a short inlet and outlet region was built to improve numerical stability (Fig. 2(*c*)). Fully developed isothermal laminar flow in an empty channel was first solved, and its flow field was applied upon the inlet boundary to enable a fully developed flow inlet. The outlet was set as "outlet" boundary (an ANSYS-CFX flow boundary condition) with the conservative mass flow rate equal to the inlet flow condition. A uniform heat flux of 5000 W/m$^2$ was applied on the fluid–solid interface, while the other faces were treated as symmetry and no-slip boundary.

**Numerical Procedure.** The modeling procedure employed for fluid transport was similar to that for heat transfer: first, idealized three-dimensional foam topology was reconstructed through Solidworks 2015™, and cubic (or spherical) nodes with various uniform sizes were created at ligament joints; second, the resulting



Downloaded From: https://heattransfer.asmedigitalcollection.asme.org on 02/14/2019 Terms of Use: http://www.asme.org/about-asme/terms-of-use

solid geometry was imported into ANSYS-ICEM 14.5™ for all tetrahedron discretization; finally, the generated meshes were imported into ANSYS-CFX 14.5™ for computations with three different boundaries and initial conditions for effective thermal conductivity, permeability, and conjugated heat transfer modeling, respectively, with double precision used for all computations. In the present simulations, relevant thermophysical properties of Al ligaments and the saturating fluid were assumed to be constant. The fluid was treated as incompressible, and steady state was assumed. The solution was thought to be converged when the residuals of all the governing equations were less than $10^{-6}$.

## Results and Discussion

**Effective Thermal Conductivity.** To validate the present direct CFD simulations, numerical results for effective thermal conductivity for air-saturated Al foam with square and circular cross-sectional areas were first compared with existing experimental data [12,20,23,24] and analytical model predictions [11] for validation (Fig. 3(*a*)). A good agreement was found. Figure 3(*b*) plotted the effective conductivity as a function of node size in dimensionless form. For a fixed porosity, a sharp decrease in thermal conductivity as the dimensionless node size α (ratio of node length to ligament thickness) was increased. For instance, the thermal conductivity was reduced by 59% when the value of α was increased from 1 to 4. Adopting the thermal tortuosity model $\tau = (1-\varepsilon)(k_s/k_e)$, $0.9 \le \varepsilon < 1$ [11], the thermal tortuosity was increased from 2.47 to 5.88 as the node size ratio α was increased from 1 to 4. This could be the direct reason underlying the decreased effective conductivity of metal foams with a fixed porosity but different node sizes.

**Permeability.** Permeability could be obtained through comparing Forchheimer-extended-Darcy model with numerically predicted pressure drop. Figure 4(*a*) showed the comparison of the predicted permeability ($\alpha = 1$) with existing data in open literature, where a reasonable good agreement was found. The results of Fig. 4(*b*) demonstrated that the permeability increased with increasing node size. For a given node shape and node-to-ligament size ratio but different ligament cross-sectional shapes (e.g., $\alpha = 4$ and spherical nodes), the permeability of a foam with circular cross-sectional ligaments was higher than that with square cross-sectional ligaments. Further, with $\alpha = 4$ and circular cross-sectional ligaments, foams with spherical nodes exhibited a higher permeability than those with cubic nodes.

**Heat Transfer Coefficient.** The conjugated heat transfer was directly evaluated by the pore-scaled Nusselt number, as

$$\mathrm{Nu}_c = \frac{h_c d_p}{k_f} \tag{1}$$

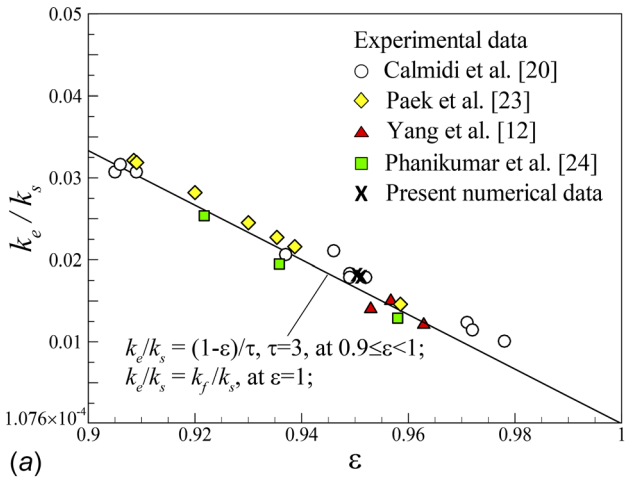


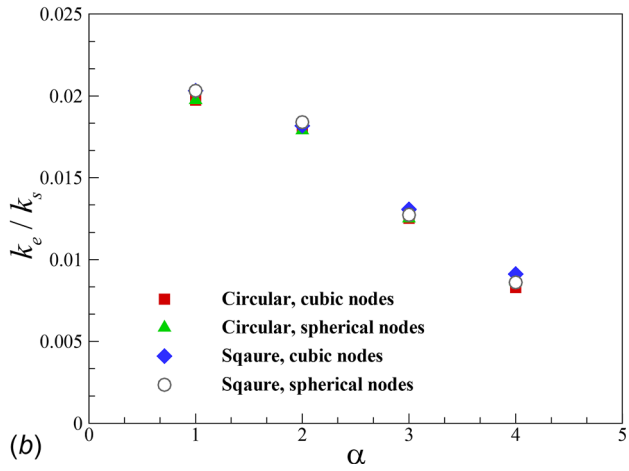


**Fig. 3 Effective thermal conductivity of open-cell metal foam: (*a*) comparison with experimental data and analytical predictions in open literature and (*b*) effect of node size**

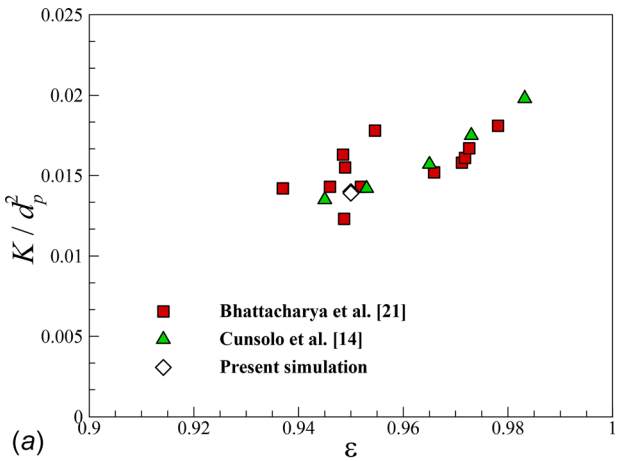


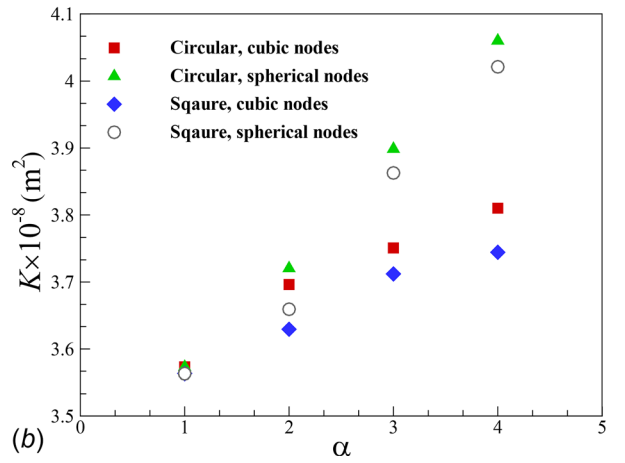


**Fig. 4 Numerically predicted permeability of open-cell metal foam: (*a*) comparison with data in open literature, with α = 1 and (*b*) plotted as a function of node size**



Downloaded From: https://heattransfer.asmedigitalcollection.asme.org on 02/14/2019 Terms of Use: http://www.asme.org/about-asme/terms-of-use

where $d_p$ was the equivalent pore diameter of open-cell foam, $k_f$ was the thermal conductivity of the cooling fluid, and $h_c$ denoted the convective heat transfer between the heating metallic ligaments and the cooling fluid. Typically, $h_c$ took the form

$$h_c = \frac{q}{\langle T_s \rangle - \langle T_f \rangle} \tag{2}$$

where $q$ was the imposed heat flux on solid ligaments, the symbol $\langle\ \rangle$ denoted volume-averaging calculation, and $T_s$ and $T_f$ were the temperature for solid ligaments and interstitial fluid, respectively. As the specific area (area-to-volume ratio) was thought to be one reason why metal foams could greatly enhance forced convective heat transfer, a modified Nusselt number that accounted for the specific area contribution was needed. Cunsolo et al. [14] suggested a volume-averaged Nusselt number ($\mathrm{Nu}_v$) as

$$\mathrm{Nu}_v = \mathrm{Nu}_c \left( \frac{S}{V} d_p \right) \tag{3}$$

where $S/V$ was the specific area of the UCs in the control volume. The Reynolds number is defined as follows:

$$\mathrm{Re} = \frac{\rho U_{\mathrm{inlet}} d_p}{\eta} \tag{4}$$

where $\rho$ and $\eta$ are the density and dynamic viscosity for the fluid, $U_{\mathrm{inlet}}$ is the mean inlet velocity, and $d_p$ denotes the equivalent pore diameter (pore size) for open-cell foam. $d_p$ can be mathematically calculated by the diameter of an equivalent sphere that occupied the same volume as the void space in a tetrakaidehedron cell.

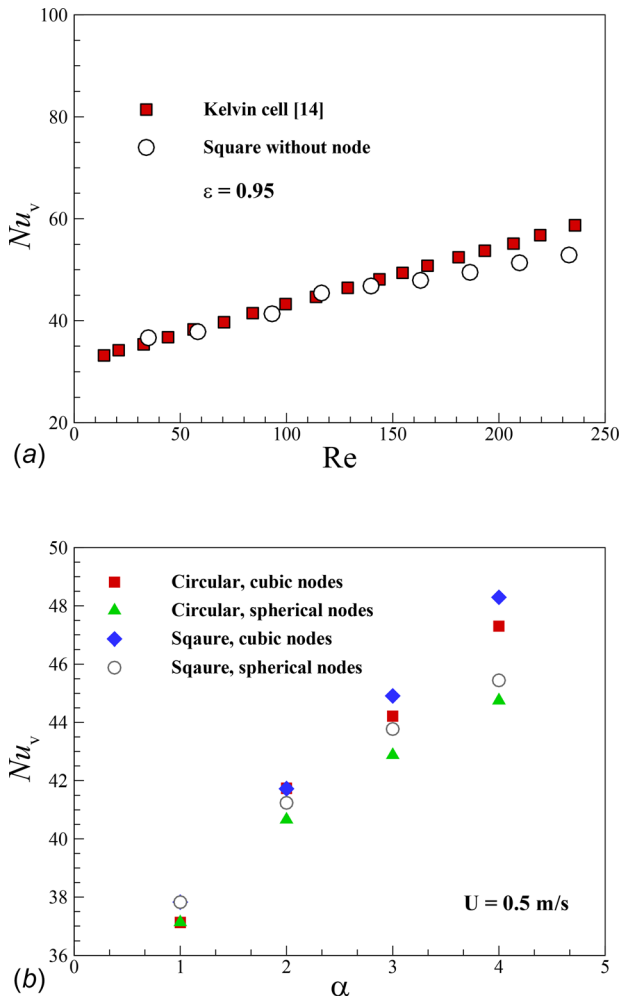


**Fig. 5 Volume-averaged Nusselt number plotted as a function of (*a*) Reynolds number and (*b*) node-to-ligament size ratio for $\varepsilon = 0.95$**

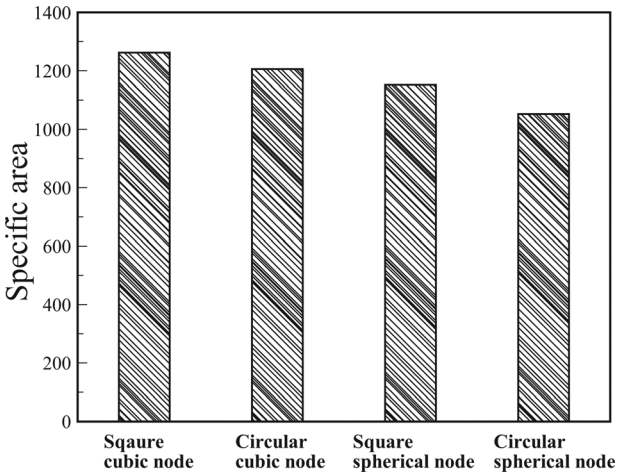


**Fig. 6 Specific area for four typical foam UCs**

Figure 5(*a*) compared the present numerical results of $\mathrm{Nu}_v$ with the numerical simulation results of Cunsolo et al. [14], with good agreement achieved. Note that Cunsolo et al. [14] employed the Kelvin cell inscribed by a sphere to simulate the convective heat transfer. Due to the inscription process, the ligaments in such cells had an irregular cross-sectional shape other than square or circular. Even so, the good agreement revealed that ligament cross-sectional shape had little influence upon convective heat transfer performance. Figure 5(*b*) plotted the volume-averaged Nusselt number as a function of node-to-ligament size ratio. It was observed that volume-averaged Nusselt number increased with increasing node size. A 27.6% and 20.5% increase was found when the node-to-ligament size ratio was increased from 1 to 4 for foam with cubic and spherical nodes, respectively. For a given node-to-ligament size ratio (e.g., $\alpha = 4$), the volume-averaged Nusselt number for the case with square ligaments and cubic nodes outperformed the other three cases. This was mainly attributed to the fact that the foam with square ligaments and cubic nodes had the largest specific area, as shown in Fig. 6. Consequently, the specific area still played a dominating role in enhancing heat transfer, even for high porosity foams. In comparison, the contribution of ligament cross-sectional shape to convective heat transfer was less significant.

## Conclusions

The effective thermal conductivity, permeability, and conjugated heat transfer of highly porous open-cell metal foams were numerically investigated. Idealized tetrakaidecahedron unit cells were periodically packed, with relatively big ligament nodes considered to better mimic the real foam geometry. The predicted results for effective thermal conductivity, permeability, and heat transfer rate agreed with experimental and numerical data in open literature, validating the method of direct simulation for fluid flow and thermal transport in open-cell metal foams.

For the studied porosity (0.95), the effective thermal conductivity was reduced by 59% when the node-to-ligament ratio increased from 1 to 4, while the permeability and volume-averaged Nusselt number increased by 16% and 27.6%. Both the node and ligament cross-sectional shape had little influence on the effective thermal conductivity, but affected significantly the permeability and volume-averaged Nusselt number. While metal foams with circular ligaments and spherical nodes exhibited the highest permeability, those with square ligaments and cubic nodes had the highest volume-averaged Nusselt number. In summary,



Downloaded From: https://heattransfer.asmedigitalcollection.asme.org on 02/14/2019 Terms of Use: http://www.asme.org/about-asme/terms-of-use

when analyzing the transport properties and conjugated heat transfer in high porosity metal foams with open cells, the effects of node size should be considered.


## Acknowledgment

The authors would like to thank Professor Oronzio Manca from Second University of Naples for constructive discussions.

## Funding Data

- Beijing Key Lab of Heating, Gas Supply, Ventilating and Air Conditioning Engineering (Grant Nos. NR2015K08 and NR2016K01).
- China Postdoctoral Science Foundation (Grant Nos. 2015M580845 and 2016T90916).
- National Natural Science Foundation of China (Grant No. 51506160).
- Shaanxi Province Post-Doctoral Science Foundation Project (Grant No. 2016BSHYDZZ54).


## Nomenclature

$d_p$ = equivalent pore diameter, m
$h_c$ = convective heat transfer coefficient between metal foam surface and interstitial fluid, W m$^{-2}$ K$^{-1}$
$K$ = permeability of metal foam, m$^2$
$k_e$ = effective thermal conductivity of open-cell metal foam, W m$^{-1}$ K$^{-1}$
$k_f$ = thermal conductivity of interstitial fluid, W m$^{-1}$ K$^{-1}$
$k_s$ = thermal conductivity of metallic ligaments, W m$^{-1}$ K$^{-1}$
$L$ = length of the computational domain along main flow direction, m
$\mathrm{Nu}_c$ = Nusselt number at pore scale
$\mathrm{Nu}_v$ = volume-averaged Nusselt number
$p$ = pressure, Pa
$p_{\mathrm{in}}$ = pressure at inlet, Pa
$p_{\mathrm{out}}$ = pressure at outlet, Pa
$q$ = imposed heat flux, W m$^{-2}$
Re = Reynolds number based on the pore-scale characteristic length
$S$ = surface area of open-cell metal foam, m$^2$
$\langle T_f \rangle$ = volume-averaged temperature of interstitial fluid, K
$\langle T_s \rangle$ = inner surface-averaged temperature of metal foam, K
$U$ = mean inlet velocity, m s$^{-1}$
$V$ = volume of the computational domain for metal foam, m$^3$
$x$ = coordinate

### Greek Symbols

$\alpha$ = node-to-ligament size ratio
$\varepsilon$ = porosity for open-cell metal foam
$\mu$ = dynamic viscosity, Pa·s
$\rho$ = density, kg m$^{-3}$
$\tau$ = thermal tortuosity

## References


[1] Lu, T. J., Stoneb, H. A., and Ashbya, M. F., 1998, "Heat Transfer in Open-Cell Metal Foams," Acta Mater., **46**(10), pp. 3619–3635.
[2] Senn, S. M., and Poulikakos, D., 2004, "Polymer Electrolyte Fuel Cells With Porous Materials as Fluid Distributors and Comparisons With Traditional Channeled Systems," ASME J. Heat Transfer, **126**(3), pp. 410–418.
[3] Amiri, A., and Vafai, K., 1994, "Analysis of Dispersion Effects and Non-Thermal Equilibrium, Non-Darcian, Variable Porosity Incompressible Flow Through Porous Media," Int. J. Heat Mass Transfer, **37**(6), pp. 939–954.
[4] Barletta, A., Celli, M., and Kuznetsov, A. V., 2013, "Convective Instability of the Darcy Flow in a Horizontal Layer With Symmetric Wall Heat Fluxes and Local Thermal Nonequilibrium," ASME J. Heat Transfer, **136**(1), p. 012601.
[5] Krishnan, S., Murthy, J. Y., and Garimella, S. V., 2005, "A Two-Temperature Model for Solid-Liquid Phase Change in Metal Foams," ASME J. Heat Transfer, **127**(9), pp. 995–1004.
[6] Feng, S. S., Kuang, J. J., Lu, T. J., and Ichimiya, K., 2015, "Heat Transfer and Pressure Drop Characteristics of Finned Metal Foam Heat Sinks Under Uniform Impinging Flow," ASME J. Electron. Packag., **137**(2), p. 021014.
[7] Zhang, Q. C., Yang, X. H., Li, P., Huang, G. Y., Feng, S. S., Shen, C., and Lu, T. J., 2015, "Bioinspired Engineering of Honeycomb Structure—Using Nature to Inspire Human Innovation," Prog. Mater. Sci., **74**, pp. 332–400.
[8] Yang, X. H., Wang, W. B., Yang, C., Jin, L. W., and Lu, T. J., 2016, "Solidification of Fluid Saturated in Open-Cell Metallic Foams With Graded Morphologies," Int. J. Heat Mass Transfer, **98**, pp. 60–69.
[9] Boomsma, K., Poulikakos, D., and Ventikos, Y., 2003, "Simulations of Flow Through Open Cell Metal Foams Using an idealized Periodic Cell Structure," Int. J. Heat Fluid Flow, **24**(6), pp. 825–834.
[10] Bai, M., and Chung, J. N., 2011, "Analytical and Numerical Prediction of Heat Transfer and Pressure Drop in Open-Cell Metal Foams," Int. J. Therm. Sci., **50**(6), pp. 869–880.
[11] Yang, X. H., Kuang, J. J., Lu, T. J., Han, F. S., and Kim, T., 2013, "A Simplistic Analytical Unit Cell Based Model for the Effective Thermal Conductivity of High Porosity Open-Cell Metal Foams," J. Phys. D: Appl. Phys., **46**(25), p. 255302.
[12] Yang, X. H., Bai, J. X., Yan, H. B., Kuang, J. J., Lu, T. J., and Kim, T., 2014, "An Analytical Unit Cell Model for the Effective Thermal Conductivity of High Porosity Open-Cell Metal Foams," Transp. Porous Media, **102**(3), pp. 403–426.
[13] Cunsolo, S., Baillis, D., Bianco, N., Naso, V., and Oliviero, M., 2016, "Effects of Ligaments Shape on Radiative Heat Transfer in Metal Foams," Int. J. Numer. Methods Heat Fluid Flow, **26**(2), pp. 477–488.
[14] Cunsolo, S., Iasiello, M., Oliviero, M., Bianco, N., Chiu, W. K., and Naso, V., 2015, "Lord Kelvin and Weaire–Phelan Foam Models: Heat Transfer and Pressure Drop," ASME J. Heat Transfer, **138**(2), p. 022601.
[15] Krishnan, S., Murthy, J. Y., and Garimella, S. V., 2006, "Direct Simulation of Transport in Open-Cell Metal Foam," ASME J. Heat Transfer, **128**(8), pp. 793–799.
[16] Krishnan, S., Garimella, S. V., and Murthy, J. Y., 2008, "Simulation of Thermal Transport in Open-Cell Metal Foams: Effect of Periodic Unit-Cell Structure," ASME J. Heat Transfer, **130**(2), p. 024503.
[17] Huu, T. T., Lacroix, M., Huu, C. P., Schweich, D., and Edouard, D., 2009, "Towards a More Realistic Modeling of Solid Foam: Use of the Pentagonal Dodecahedron Geometry," Chem. Eng. Sci., **64**(24), pp. 5131–5142.
[18] Lucci, F., Della Torre, A., von Rickenbach, J., Montenegro, G., Poulikakos, D., and Eggenschwiler, P. D., 2014, "Performance of Randomized Kelvin Cell Structures as Catalytic Substrates: Mass-Transfer Based Analysis," Chem. Eng. Sci., **112**, pp. 143–151.
[19] Zafari, M., Panjepour, M., Meratian, M., and Emami, M. D., 2016, "CFD Simulation of Forced Convective Heat Transfer by Tetrakaidecahedron Model in Metal Foams," J. Porous Media, **19**(1), pp. 1–11.
[20] Calmidi, V. V., and Mahajan, R. L., 1999, "The Effective Thermal Conductivity of High Porosity Fibrous Metal Foams," ASME J. Heat Transfer, **121**(2), pp. 466–471.
[21] Bhattacharya, A. A., Calmidi, V. V., and Mahajan, R. L., 2002, "Thermophysical Properties of High Porosity Metal Foams," Int. J. Heat Mass Transfer, **45**(5), pp. 1017–1031.
[22] Boomsma, K., and Poulikakos, D., 2001, "On the Effective Thermal Conductivity of a Three-Dimensionally Structured Fluid-Saturated Metal Foam," Int. J. Heat Mass Transfer, **44**(4), pp. 827–836.
[23] Paek, J. W., Kang, B. H., Kim, S. Y., and Hyun, J. M., 2000, "Effective Thermal Conductivity and Permeability of Aluminum Foam Materials," Int. J. Thermophys., **21**(2), pp. 453–464.
[24] Phanikumar, M. S., and Mahajan, R. L., 2002, "Non-Darcy Natural Convection in High Porosity Metal Foams," Int. J. Heat Mass Transfer, **45**(18), pp. 3781–3793.





Downloaded From: https://heattransfer.asmedigitalcollection.asme.org on 02/14/2019 Terms of Use: http://www.asme.org/about-asme/terms-of-use